Author's Accepted Manuscript

Plastic yielding and tensile strength of near-micrometer grain size pure iron

Qing Ruan, Muxin Yang, Wei Liu, Andy Godfrey

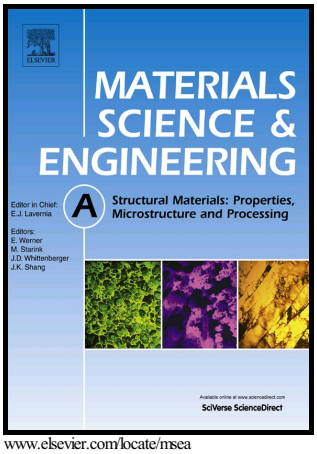

www.elsevier.com/locate/msea

PII: S0921-5093(18)31734-9
DOI: https://doi.org/10.1016/j.msea.2018.12.056
Reference: MSA37328

To appear in: *Materials Science & Engineering A*

Received date: 13 February 2018
Revised date: 11 December 2018
Accepted date: 12 December 2018

Cite this article as: Qing Ruan, Muxin Yang, Wei Liu and Andy Godfrey, Plastic yielding and tensile strength of near-micrometer grain size pure iron, *Materials Science & Engineering A,* https://doi.org/10.1016/j.msea.2018.12.056

This is a PDF file of an unedited manuscript that has been accepted for publication. As a service to our customers we are providing this early version of the manuscript. The manuscript will undergo copyediting, typesetting, and review of the resulting galley proof before it is published in its final citable form. Please note that during the production process errors may be discovered which could affect the content, and all legal disclaimers that apply to the journal pertain.

ACCEPTED MANUSCRIPT

Plastic yielding and tensile strength of near-micrometer grain size pure iron

Qing Ruan[1], Muxin Yang[2], Wei Liu[1], Andy Godfrey[1*]

[1]Laboratory of Advanced Materials, School of Material Science and Engineering, Tsinghua University, Beijing 100084, PR China

[2]State Key Laboratory of Nonlinear Mechanics, Institute of Mechanics, Chinese Academy of Sciences, Beijing 100190, PR China

[*]Corresponding author: awgodfrey@mail.tsinghua.edu.cn

Accepted manuscript

Abstract

In order to investigate the influence on mechanical properties of grain size in the near-micrometer regime, samples of Fe with nearly full density were prepared using the spark plasma sintering (SPS) technique with average grain sizes of 1.0 μm, 2.6 μm and 4.0 μm. In each of these samples the resulting sintered material was in a nearly fully-recrystallized condition with a random texture. The mechanical properties of the samples were examined via tensile testing. A strong dependence of the tensile flow characteristics on the average grain size was observed in this size regime, with the 1.0 μm grain-size sample showing a very high strength, but no uniform elongation and a large yield drop developed in the 2.6 μm grain-size sample. Analysis of the grain size dependence of yield strength suggests a positive Hall-Petch deviation from the expected grain boundary strengthening in the SPS Fe samples, assuming a typical range of values for the grain boundary strength (Hall-Petch coefficient). Pre-compression of the 2.6 μm

ACCEPTED MANUSCRIPT

grain-size prior to tensile testing sample results in a removal of the yield drop and a corresponding large decrease in the yield stress by as much as 145 MPa. The observations suggest that the positive Hall-Petch deviation seen previously in the near-micrometer regime for fully recrystallized Al and Cu may also be present in Fe, and highlight the likely importance of dislocation source hardening in this grain size regime.

Keywords: electron microscopy; stress/strain measurements; EBSD; iron alloys; spark plasma sintering.

1. Introduction

Some unique mechanical properties of metals with a microstructural scale in the near-micrometer regime have been reported in a number of studies, including the presence of a yield drop [1-5], hardening by annealing [6], and a positive deviation from the Hall-Petch relationship for boundary strengthening [7]. These observations have mainly been explored in metals prepared by severe plastic deformation, followed by annealing. The unusual mechanical properties in such metals are very clear. There are, however, some complications in relating the microstructural origin of these phenomena, as such as such near-micrometer grain size metals generally contain a significant population of low angle dislocation boundaries, and may be better thought of as recovered deformation microstructures than as recrystallized grain structures [8-11].

To avoid these complications the spark plasma sintering (SPS) process [12], also referred to by some authors as the field assisted sintering technique (FAST), which has been used in recent years for the synthesis of a wide range of metals and alloys [13-15], has been proposed as an alternative method for preparation of samples with grain sizes in the near-micrometer regime [16-20]. It has been shown that both for Al and Cu this process allows the preparation of samples

Accepted manuscript

ACCEPTED MANUSCRIPT

in a nearly fully recrystallized condition, and that the resulting materials exhibit yield strengths larger than predicted based on the conventional Hall-Petch parameters for these metals [19,20]. Similar results, have been obtained in cases where it has proven possible to obtain a sufficiently fine recrystallized grain size by deformation followed by annealing [21-23]

The presence of a yield-point is of course well established and a much studied phenomenon in both Fe and steel, where this is most commonly attributed to a lack of mobile dislocations due to pinning by interstitial solutes [24-26]. It is of interest therefore to investigate both whether it is possible to achieve fully-recrystallized near-micrometer grain sizes in pure Fe, and whether such samples show the enhanced yield strength (positive Hall-Petch deviation) seen in Cu and Al samples. Study of spark plasma sintered Fe may also overcome some complications in analysis of the origin of the enhanced yield strength in near-micrometer grain size samples. In particular in Al samples prepared by SPS a highly dense network of 20 – 50 nm diameter oxides is present at the grain boundaries (at a 3 – 4% volume fraction for the finest grain size samples) [19], resulting from the transformation during the SPS process of the native alumina layer on the initial powders. In addition to restricting grain growth, these nanoscale oxide particles may also provide some additional hardening via an Orowan mechanism. Previously reported investigations on the sintering of nanoscale Fe powders and Fe powders processed by high energy ball milling have shown that such a dense network of grain boundary nanometer-size oxide particles is not found in SPS-sintered Fe samples [27-29]. This is supported by the observation in the present study that the grain size increases with sintering temperature (in the Al samples the nanoscale oxide particles prevent any grain growth up to temperatures near the melting point). Similarly, in Cu SPS samples a large fraction of twin boundaries are developed, which may or may not be regarded as having similar mechanical properties to general boundaries

Accepted manuscript

ACCEPTED MANUSCRIPT

(the choice of which results in a significant difference in the determined "grain" size) [20], whereas in Fe a high density of annealing twins is not expected.

In Al a range of fine grain sizes can be obtained by SPS of powders with different average particle size (as the grain size is largely determined by the powder size as a result of the surface oxides) [19]. In Cu, such an effect does not exist and the SPS temperature has been used to control grain size [20]. For the Fe samples of the current study it has been found that use of both different powders and sintering conditions has been necessary to achieve suitable range of near-micrometer grain sizes.

2. Experimental Methods

Atomized pure Fe powders (Beijing Dk Nano Technology Co., Ltd) were used to prepare the SPS samples. To obtain the desired range of grain sizes three different powder sizes were used, in each case with a purity of 99.9%. Example scanning electron microscope (SEM) images of the three powders are shown in Fig. 1a-c. All the powders exhibited a unimodal distribution of powder size, with particle diameters in the range 0.5 - 1 μm (powder P1) , 1 - 3 μm (powder P2), and 8 - 10 μm (powder P3). All powders used in this research were kept in a drying closet prior to sintering. The powder composition, as supplied by the manufacturer, is given in Table 1. In addition, as a control sample of coarse grain size Fe prepared by a non-SPS route, rolled electrolytic pure Fe (Beijing Trillion Metals Co., Ltd.), annealed at 650 °C for 190 min to achieve a fully recrystallized condition was also examined.

Sintering of the samples was carried out using a SPS-1050 instrument (Sumitomo Coal Mining Co., Ltd). In each case 10 g of powder was packed in a 20 mm diameter graphite die. To prevent diffusion of carbon into the samples a layer of tantalum foil was used at the inner surface of the

Accepted manuscript

ACCEPTED MANUSCRIPT

die. The die was then placed into the sintering chamber and stabilized under an initial pressure of 20 MPa during which time the chamber was evacuated. After a suitable vacuum was reached, the sintering cycle was commenced using a heating rate of 100 °C/min up to a temperature 50 °C below the target sintering temperature (T_s). The final 50 °C temperature increase to reach Ts was achieved using a heating rate of 50 °C/min. Once at the sintering temperature the load was increased to 60 MPa, and held for 1 min, after which the load and the vacuum were released and the sample allowed to air-cool to room temperature. The temperature during sintering was controlled by a thermocouple inserted into a hole in the die, and in contact with the sample.

For each sample the average density was determined by Archimedes' method, using absolute ethyl alcohol after grinding all surfaces up to 1500-grit SiC. Results are given here as the average of measurements on three samples. The microstructure and texture of the samples were investigated in a scanning electron microscope (SEM; Tescan 5136XM or Zeiss Supra 35), equipped with an Oxford Instruments electron backscatter diffraction (EBSD) system. All investigations were made on electro-polished samples of size 1 mm thickness, 5 mm in width and 5 mm in length prepared using 10% $HClO_4$+90% C_2H_5OH solution at a voltage of 25V. Post-processing and analysis of the EBSD data was carried out using the Oxford Instruments Channel 5 software package, as well as using in-house software [30]. The grain size of each sample was determined from the EBSD data using boundary misorientation angle definitions of 15° and 2°. For analysis of the microstructure-property relationship grain sizes using the 2° definition were used. This choice was based on previous studies showing that dislocation boundaries with angles as low this value can act as grain boundaries, with boundaries of lower misorientation angle providing strengthening instead through a Taylor (square root of dislocation density) relationship [7,31]. For all EBSD maps a minimal amount of data cleaning was used,

Accepted manuscript

ACCEPTED MANUSCRIPT

consisting of wild-spike correction followed by three rounds of zero-solution correction using a setting of 5 out of 8 neighbors.

The mechanical properties of the samples were evaluated using tensile testing carried out at room temperature. Due to the small size of the sintered disks a reduced-size dog-bone shaped specimen, with a gauge length, width, and thickness of 8 mm, 2 mm, and 1 mm, respectively was used, based on a scaled-down version of the dimensions recommended in ASTM E8/E8M-09. Tensile blanks were cut using spark erosion, and the surfaces ground to SiC 3000 grit before testing. Samples were tested to failure in an Instron-5966 testing machine under displacement control at an initial strain rate of 8×10^{-4} s^{-1} with three samples tested for each grain size. The strain was measured during tensile testing using a strain gauge of length 5 mm. The morphology of each fracture surface was observed in a SEM. It can be additionally noted that all microstructural observations were made on interior surfaces, and the way the tensile blanks were cut ensured that the gauge volume was located at least 2 mm from the surface of the sintered disks. It can be noted that based on a time of 5 mins at 730°C (for ferrite) and 1000°C (for austentite) the approximate diffusion distance is only a few micrometers for Ta based on a simple $\sqrt{(Dt)}$ calculation using values for the diffusion coefficient taken from Shaikh [32]).

Accepted manuscript

3. Results

3.1 Sample synthesis parameters

In this study the main goal is the investigation of the mechanical properties of near-micrometer grain size Fe. As such we present here only a summary of the synthesis parameters used to obtain suitable samples for this purpose. A more detailed investigation of the dependence of microstructure on SPS parameters will be given in a forthcoming paper. For powder P1 (the

ACCEPTED MANUSCRIPT

finest powder size used) samples were sintered at temperatures of between 650 °C and 950 °C in 100 °C increments. The measured density and selected grain size values are given in Table 2. At 750 °C and above a stable density of ≈ 97.5% is achieved, with a large increase in grain size between 750 °C and 850 °C (confirming that highly dense boundary oxide networks do not form in SPS Fe samples). For powder P1 the chosen sintering condition was taken therefore as 750 °C for 1 min, to give a sample with grain size based on a 2° misorientation angle definition of d_{2° = 1.0 μm . For powder P2 an initial sintering test under the same conditions (750 °C for 1 min) yielded a sample with a density of ≈ 97.9% and a suitable grain size of d_{2° = 2.6 μm.

For powder P3, with a more irregular particle shape and larger particle size, sintering was carried out at temperatures between 750 °C and 1000 °C in increments of 50°C. The sample selected for investigation in this study was that sintered at 1000 °C, with a grain size of d_{2° = 4.0μm and a density of ≈ 96.4% (see Table 2)

3.2 Microstructural characterization

Example EBSD images showing the microstructure of the SPS samples selected for investigation in this study are shown in Fig. 2(a-c), while figure 2(d) shows the microstructure of the coarse grain Fe sample prepared by annealing of rolled electrolytic Fe sheet. In these maps black lines represent misorientations greater than 15°, with misorientations in the range 2° to 15° shown in silver. The color in the EBSD maps represents the crystal direction parallel to the loading axis during sintering, in inverse pole figure coloring, and is superimposed on a EBSD band contrast map. The images show that in each case the microstructure is dominated by grains surrounded by high angle boundaries, with little evidence of internal deformation. In the SPS samples the grain shapes are slightly irregular in the samples with the larger grain sizes of 2.6 μm and 4.0 μm, with

Accepted manuscript

ACCEPTED MANUSCRIPT

a more equiaxed morphology in the sample with a grain size of 1.0 μm. The rolled and annealed electrolytic Fe sample also had slightly irregular grain morphology, with the grain size determined as d_{2° = 33 μm.

The nearly random texture suggested by the coloring in the EBSD maps for the SPS samples is confirmed by inspection of plots of the misorientation angle distribution (Fig. 3a-d), plotted here using a lower angle cut-off of 2°, where the shape closely matches that of the Mackenzie distribution [33] expected for a fully random distribution of grains in the case of cubic crystal symmetry. Further evidence for the nearly random texture is provided by inspection of {111} pole figures (see Supplementary Material), where a maximum intensity of only 1.74 is found. Note that the step-sizes and mapping areas for the EBSD maps were chosen such that data for each sample covers more than 1500 grains. The measurements can be assumed therefore to be sufficiently representative of the bulk texture according to previous studies where it has been shown that the texture in EBSD data can be adequately described by a minimum of 1000 grains [34].

The fractions of misorientations less than 15° for the four samples are 8% (1.0 μm), 5% (2.6 μm), 11% (4.0 μm), and 9% (33 μm). The peak in the misorientation distribution for the rolled and annealed electrolytic Fe sample is due to the presence of a number of twin boundaries in the microstructure for this deformed plus annealed sample (shown in red in Fig. 2).

As a more thorough check on the extent to which the samples can be regarded as fully recrystallized, maps were also constructed showing separately the misorientation axis, in the sample reference frame (${}^{s}\mathbf{r}_{pix,av} = {}^{s}[uvw]_{pix,av}$), and the misorientation angle of each pixel to the average grain orientation ($\theta_{pix,av}$). It has been demonstrated elsewhere [30,35,36] that such maps

Accepted manuscript

ACCEPTED MANUSCRIPT

provide a very sensitive method to visualize small orientation differences arising even from very low amounts of plastic strain. These maps were calculated using in-house software (available on request from the corresponding author).

The resulting maps for the investigated samples are shown in Fig. 4(a-h). In Fig. 4(a-d) the misorientation angle of each pixel to the grain average ($\theta_{pix,av}$) is shown on a color scale from pure yellow at $\theta_{pix,av} = 0°$ to pure blue at $\theta_{pix,av} = 2°$, with green indicating pixels with $\theta_{pix,av} > 2°$. The misorientation angle maps show that almost all the grains in the 1μm grain-size sample, and a large majority of the grains in the other samples, show a very small extent of in-grain orientation variation, with the largest extent of in-grain orientation variation seen in the 4μm grain-size sample. This is confirmed by inspection of the ${}^{s}\mathbf{r}_{pix,av}$ maps (Fig. 4e-h). In these maps, regions of finely varying mixed color correspond to areas where the misorientation axis varies randomly, indicating no systematic in-grain rotation, whereas a region of similar color indicates a part of a grain that is rotated with respect to the grain average. Based on the microstructural observations it is concluded that the samples satisfy the requirements outlined earlier, of having grain sizes in near-micrometer regime, with a close to random texture and in a predominantly fully recrystallized condition.

Accepted manuscript

3.3 Tension testing

Example stress-strain curves from tensile tests of the selected samples are shown in Fig. 5. The curves show a similar pattern to samples of Al [19] and Cu [20] with near-micrometer grain size. The finest grain-size sample ($d_{2°}$ = 1.0 μm) shows a very high yield strength of 695 ± 29 MPa but no uniform elongation in all three samples tested (note that values for mechanical data given in this section are given as average and standard deviation based on measurements on three

ACCEPTED MANUSCRIPT

samples). The SPS sample with a grain size of $d_{2°}$ = 2.6 μm shows a large yield drop (upper yield point of 601 ± 60 MPa), followed by an extended region of flow instability typically associated with Lüders band deformation, and then by rapid work-hardening, resulting in an overall uniform ductility of 12.1 ± 0.6 %. The 4.0 μm grain size sample shows a much smaller yield drop (upper yield point of 495 ± 21 MPa) followed by a flow plateau (more typical of that seen in samples of annealed Fe), and then a similar work-hardening and uniform elongation (12.4 ± 0.5 %) to the 2.6 μm grain size sample. The rolled and annealed electrolytic Fe sample, with a grain size of $d_{2°}$ = 33 μm shows a very mild yield drop (upper yield point of 196 ± 12 MPa), followed by much lower work hardening than seen in the near-micrometer grain size SPS samples with a uniform elongation of 19.3 ± 0.9 %.

Fracture surfaces of the samples as seen from SEM observations are shown in Fig. 6. Some evidence of the original powder is seen in the 2.6 μm grain size sample, but in general a large area showing dimples is observed in each case, with no evidence of cleavage cracks, indicating therefore failure predominantly by a ductile mode in all samples.

4. Discussion

4.1 Grain size control in Fe prepared by SPS

For all three powders the grain sizes in the high-density sintered condition are comparable, though a little smaller, to the powder particle sizes. Direct comparison is however complicated for powder P1 by extensive particle agglomeration, and by the non-uniform shapes in powder P3. The observations confirm nevertheless that control of grain size in the near-micrometer regime can be achieved at least in part by appropriate powder particle selection. Sintering of powder P1

Accepted manuscript

ACCEPTED MANUSCRIPT

at 850 °C results in a large increase in grain size (see Table 2), suggesting that highly dense networks of nanoscale oxides, as seen in previously studied Al SPS samples, are not present in samples sintered from Fe powders, Additionally the as-sintered SPS samples contain only a small fraction of twin boundaries (approximately 3% of the total boundary length, based on a 2° boundary angle definition), so that the grain sizes determined from the EBSD data are unaffected, within the experimental error of the data, by the choice of whether to count twin boundaries as grain boundaries or not.

Microstructural investigations also show that the grains in the fully dense samples are largely in a fully recrystallized condition, as evidenced both by the texture and misorientation distribution, and by the low levels of internal misorientation variation within each grain, as seen from the deviation to average axis and angle maps (Fig. 4). The high sensitivity of these maps is illustrated by the fact that these maps also pick up residual deformation in the rolled and annealed sample (Fig. 4d,h) arising from sample preparation, even though this is not visible in band contrast maps or in misorientation angle maps, due to the very small levels of plastic deformation involved.

The slightly higher levels of in-grain orientation variation in the 4.6 μm sample are likely to be associated with the significantly higher sintering temperature for this sample (1000 °C). In addition to the increased relative softness of the material under the applied sintering of 60 MPa, the observed in-grain orientation variations may also result from the transformation from the γ to α phase on cooling from a temperature significantly higher than the Ac3 temperature (this transformation may also account for the more irregular grain shapes in this sample).

Accepted manuscript

ACCEPTED MANUSCRIPT

4.2 Mechanical properties in the near-micrometer grain size regime

The mechanical properties under tensile testing of the Fe-SPS samples are similar to those observed previously for both SPS-Al and SPS-Cu with near-micrometer grain sizes. In each case a transition from high strength with almost no ductility to a flow curve exhibiting an extensive yield-drop takes place as the grain size is increased in the near-micrometer regime. The mechanical properties are analyzed further in the Hall-Petch plot of Fig. 7 where the yield stress is plotted as a function of inverse square root of the grain size. In this plot the value of yield stress is taken as the UTS for 1.0 μm grain size sample (close to a 0.2% offset stress value), and as the upper yield point for the other samples. Also shown in Fig. 7 is a solid line corresponding to an extrapolation to the fine grain size regime of the Hall-Petch slope for Fe (k_{HP} = 330 MPaμm$^{0.5}$) taken from a recent review paper [37], where it can be seen that the data for the fine-grained SPS samples all show strengths well above predicted values.

A complication, however, in assessing the mechanical properties of the Fe SPS samples is the large range of Hall-Petch parameters that have been reported in individual studies, where it is found that both the chemical composition, extent of grain boundary segregation and processing treatment may all affect the measured values [38-40]. Values of the grain boundary strength (i.e. k_{HP}) have been reported ranging from as low as k_{HP} = 120 MPaμm$^{0.5}$ [1] or 150 MPaμm$^{0.5}$ [41] in IF-steel, and k_{HP} = 206 MPaμm$^{0.5}$ in decarburized ARMCO iron [42], to up to k_{HP} = 740 MPaμm$^{0.5}$ for mild steel [43]. Morrison [44], in contrast reported an almost fixed value of k_{HP} = 600 MPaμm$^{0.5}$ for mild steels with C content ranging from 0.005 – 2%.

Moreover, it has also been suggested that for a given alloy the extent of grain boundary segregation of interstitial elements (in particular for C) can have a large effect of the measured

ACCEPTED MANUSCRIPT

value of the boundary strength. Mintz et al. [45], for example, reported that the measured grain boundary strengths in a low carbon steel were k_{HP} = 315 MPaμm$^{0.5}$ and k_{HP} = 725 MPaμm$^{0.5}$ for ice-quenched and furnace-cooled samples, respectively, and the that increase in boundary strength was accompanied by an increase in grain boundary carbon segregation, based on 3-dimensional atom probe (3DAP) investigations. Alternatively it has been proposed that the both Cottrell atmosphere strength and grain boundary segregation may be influenced cooling rate, and that the former is more important in controlling the measured Hall-Petch parameters, via its influence on the extent of discontinuous yielding [46].

Given the wide variation in reported the dependence of yield stress on grain size, dashed lines in Fig. 7 show extrapolations to the fine grain size regime for a number of Hall-Petch parameters. Only for k_{HP} = 740 MPaμm$^{0.5}$ (close to the value for mild steel) do the values for the current Fe SPS samples lie close to, or below, the predicted values: in all other cases some additional hardening (i.e. a positive deviation from a Hall-Petch relationship) is inferred from the SPS Fe data falling consistently above the predicted values. The results suggest therefore that the additional strengthening seen in samples of Al and Cu for near-micrometer grain sizes may also be present for Fe, though it is not possible without a detailed investigation of chemical composition and boundary segregation to determine the extent of the positive Hall-Petch deviation. It can be noted additionally that except for the case of gas-filled pores or finely dispersed nanosize voids [47], any porosity in the sample can only reasonably be expected to lead to an underestimate of the yield strength, as measured in tension so that the analysis above is not affected by the small amount of porosity indicated from the density measurements.

Accepted manuscript

ACCEPTED MANUSCRIPT

In the previously studied Al and Cu samples it has been postulated [6,7,19,20] that origin of the positive Hall-Petch deviation is a lack of a sufficient density of dislocation sources in fine fully-recrystallized grains to provide macroscopic yielding, i.e. in such grains there is a low probability of sources that can operate, and/or of dislocation interactions leading to the generation of new sources. In samples where recovery annealing has been used to lower the dislocation density this phenomenon has been referred to as hardening by annealing [6]. In Fe a similar effect is well established (and implemented industrially as temper rolling), where removal of the yield point results in a transition to continuous flow accompanied by a reduction in the flow stress [48-50]. In this case the effect of the additional deformation is generally regarded is being related to the introduction of a sufficient density of mobile dislocations (i.e. unpinned by Cottrell atmospheres) [24].

The influence of such pre-deformation is tested in the present case by providing pre-compression of a few percent deformation to tensile samples of the 2.6 μm grain-size Fe SPS material, with the pre-compression either perpendicular to tensile axis (loading applied to the flat-face of the dog-bone sample) or along the tensile axis. The effect is strongly dependent on the pre-loading (Fig. 8), but in both cases the additional deformation results in a removal of the yield drop and a large reduction in the yield stress. In the case of the pre-deformation along the tensile axis, the work hardening of the sample follows closely that of the as-sintered sample, whereas for the sample pre-loaded perpendicular to the tensile axis shows a modified work-hardening pattern.

The magnitude of the reduction in yield stress (145 MPa; representing 22% of the yield strength in the as-SPS condition) larger than that typically seen in studies of the deformation of Fe and mild steel [48-50]. It should be recalled however that few data exist in the literature regarding the behavior of Fe with very fine recrystallized grain size, for the reasons discussed at the start of

Accepted manuscript

ACCEPTED MANUSCRIPT

this paper. As such, although not conclusive the size of the decrease in yield stress with pre-compression is consistent with an explanation relating a positive deviation from the expected Hall-Petch strength of the as-sintered SPS Fe samples to the recrystallized nature (and hence low dislocation density) of the grains in these samples. Although a positive deviation from the Hall-Petch relationship has also been reported in samples with a ultra-fine grain size prepared by annealing of severe plastic deformation methods [7], in these samples the amount of additional hardening is limited as in many cases they are essentially recovered deformation microstructures rather than grain structures resulting from recrystallization with a low associated dislocation density.

Another interesting observation is the much higher work hardening rate (and strain hardenability) for the 2.0 μm and 4.6 μm grain size samples compared to the coarse grain material. The origins of this behavior remain to be explored in detail and are the subject of ongoing studies. It is tentatively suggested however that for samples with a grain size distribution in the near-micrometer regime the presence of fine (less than 1 μm) grains can act as locally hard volumes, leading to enhanced mechanical incompatibility, as seen for example in materials with heterogeneous and gradient microstructures [51-53].

Accepted manuscript

5. Summary and conclusions

Samples of Fe in a fully recrystallized condition and with grain sizes in near-micrometer range have been successfully prepared by the use of spark plasma sintering. The mechanical properties of these samples have been examined and a strong dependence on the tensile flow characteristics is observed as the average grain size is reduced from 4.6 μm to 1 μm, matching that seen previously for samples of FCC metals in Al and Cu. The finest grain size (1.0 μm) sample shows

ACCEPTED MANUSCRIPT

very high strength but almost no ductility. Increase of grain size to 2.6 μm results in development of a very large yield drop followed by a Lüders-like flow instability. A similar behavior is seen for samples with 4.0 μm grain size, albeit with a much smaller yield drop. Both samples show high post-Luders work-hardening rate. Analysis of the grain size dependence of the flow stress is complicated by the wide range of Hall-Petch parameters reported for Fe (dependent on composition, boundary chemistry and processing treatment). The data for the near-micrometer grain size Fe only fall close to, or below, the predicted values taking Hall-Petch parameters comparable to those for mild steel (k_{HP} of 740 MPaμm$^{0.5}$). Given the initial power purity and SPS processing conditions, it is therefore concluded that a positive deviation from a Hall-Petch relationship may exist for Fe in the near-micrometer regime, but that it is difficult to quantify the magnitude of this deviation as a result of the sensitivity of the grain boundary strength to the exact composition and grain boundary chemistry. For the 2.6 μm grain size sample a small compressive pre-deformation to the tensile sample results in a complete removal of the yield-drop and a large decrease in the yield strength of up to 145 MPa. The magnitude of this decrease is consistent with an explanation that a positive deviation from the expected Hall-Petch strength for samples with grain size in the near-micrometer regime is related to the fully recrystallized nature of the grains. Further work, including detailed studies of boundary chemistry using the 3DAP technique and efforts to achieve samples with sub-micrometer grain sizes in a fully recrystallized condition should shed further light on these topics, and with the mechanical behavior of near-micrometer grain size samples providing another prism into the yielding and plastic deformation of Fe.

Accepted manuscript

ACCEPTED MANUSCRIPT

Acknowledgements

Financial support from the National Natural Science Foundation of China under project numbers 51671113 (QR, WL, AG) and 51601204 (MXY) is gratefully acknowledged.

Data availability

The mechanical and microstructural data included in this paper are available upon request from the corresponding author.

References

[1] N. Tsuji, Y. Ito, Y. Saito, Y. Minamino, Strength and ductility of ultrafine grained aluminum and iron produced by ARB and annealing, Scr. Mater. 47 (2002) 893.

[2] C.Y. Yu, P.W. Kao, C.P. Chang, Transition of tensile deformation behaviors in ultrafine-grained aluminum. Acta Mater. 53 (2005) 4019.

[3] P.C. Hung, P.L. Sun, C.Y. Yu, P.W. Kao, C.P. Chang, Inhomogeneous tensile deformation in ultrafine-grained aluminum, Scr. Mater. 53 (2005) 647-652.

[4] P.L. Sun, E.K. Cerreta, G.T. Gray, J.F. Bingert, The effect of grain size, strain rate, and temperature on the mechanical behavior of commercial purity aluminum, Metall. Mater. Trans. 37A (2006) 2983.

[5] O. Saray, G. Purcek, I. Karaman, H.J. Maier, Improvement of formability of ultrafine-grained materials by post-SPD annealing. Mater. Sci. Eng. A 619 (2014) 119.

Accepted manuscript

ACCEPTED MANUSCRIPT

[6] X. Huang, N. Hansen, N. Tsuji, Hardening by annealing and softening by deformation in nanostructured metals, Science 312 (2006) 249.

[7] N. Kamikawa, X. Huang, N. Tsuji, N. Hansen, Strengthening mechanisms in nanostructured high-purity aluminium deformed to high strain and annealed, Acta Mater. 57 (2009) 4198-4208.

[8] N. Kamikawa, N. Tsuji, X. Huang, N. Hansen, Quantification of annealed microstructures in ARB processed aluminum, Acta Mater. 54 (2006) 3055-3066.

[9] O.V. Mishin, A. Godfrey, D. Juul Jensen, N. Hansen, Recovery and recrystallization in commercial purity aluminum cold rolled to an ultrahigh strain, Acta Mater. 61 (2013) 5354-5364.

[10] F. Wetscher, R. Pippan, Cyclic high-pressure torsion of nicker and Armco iron, Phil. Mag. 86 (2006) 5867-5883.

[11] S. Gao, M. Chen, M. Joshi, A, Shibata, N. Tsuji, Yielding behavior and its effect on uniform elongation in IF steel with various grain sizes, J. Mater. Sci. 49 (2014) 6536-6542.

[12] M. Omori, Sintering, consolidation, reaction and crystal growth by the spark plasma system (SPS), Mater. Sci. Eng. A 287 (2000) 183-188.

[13] R. Zheng, F. Ma, W. Xiao, K. Ameyama, C. Ma, Achieving enhanced strength in ultrafine lamellar structured Al2024 alloy via mechanical milling and spark plasma sintering, Mater. Sci. Eng. A 687 (2017) 155-163.

[14] F. Deirmina, M. Pellizzari, M. Federici, Production of a Powder Metallurgical Hot Work Tool Steel with Harmonic Structure by Mechanical Milling and Spark Plasma Sintering, Metal. Mater. Trans. A 48 (2017) 1910-1920.

Accepted manuscript

ACCEPTED MANUSCRIPT

[15] P.N. Browning, S. Alagic, B. Carroll, A. Kulkarni, L. Matson, J. Singh, Room and ultrahigh temperature mechanical properties of field assisted sintered tantalum alloys, Mater. Si. Eng. A 680 (2017) 141-151.

[16] G.D. Dutel, P. Langlois, D. Tingaud, G. Dirras, Room-temperature deformation micro-mechanisms of polycrystalline nickel processed by spark plasma sintering, Mater. Charact. 79 (2013) 76-83.

[17] G. Marnier, C. Keller, J. Noudem, E. Hug, Functional properties of a spark plasma sintered ultrafine-grained 316L steel, Mater. Des. 63 (2014) 633-640.

[18] M. Kubota, B.P. Wynne, Electron backscattering diffraction analysis of mechanically milled and spark plasma sintered pure aluminium, Scripta Mater. 57 (2007) 719-722.

[19] G.M. Le, A. Godfrey, N. Hansen, Structure and strength of aluminum with sub-micrometer/micrometer grain size prepared by spark plasma sintering, Materials & Design 49 (2013) 360-367.

[20] K.N. Zhu, A. Godfrey, N. Hansen, X.D. Zhang, Microstructure and mechanical strength of near- and sub-micrometre grain size copper prepared by spark plasma sintering, Materials & Design 117 (2017) 95-103.

[21] Y.Z. Tian S. Gao, L.J. Zhao, S. Lu, R. Pippan, Z.F. Zhang, N. Tsuji, Remarkable transitions of yield behavior and Luders deformation in pure Cu by changing grain sizes, Scr. Mater. 132 (2018) 88-91

Accepted manuscript

ACCEPTED MANUSCRIPT

[22] Y.Z. Tian, L.Z. Zhao, S. Chen, D. Terada, A. Shibata, N. Tsuji, Optimizing strength and ductility in Cu–Al alloy with recrystallized nanostructures formed by simple cold rolling and annealing, J. Mater. Sci. 49 (2014) 6629-6639.

[23] S. Yoshida, T. Bhattarcharjee, Y. Bai, Friction stress and Hall-Petch relationship in CoCrNi equi-atomic medium entropy alloy processed by severe plastic deformation and subsequent annealing, Scr. Mater. 134 (2017) 33-36.

[24] A. H. Cottrell, B. A. Bilby, Dislocation theory of yielding and strain ageing of iron, Proc. Phys. Soc. A 62 (1949) 49-62.

[25] J. R. Low, M. Gensamer, Aging and the yield point in steel, Trans. American Institute of Mining and Metallurgical Engineers, 158 (1944) 207-242.

[26] D. J. Dingley, D. McLean, Components of the flow stress of iron, Acta Metall. 15 (1967) 885-901.

[27] Y. Ye, X. Li, Z. Cheng, M. Zhang, S. Qu, The influence of sintering temperature and pressure on microstructure and mechanical properties of carbonyl iron powder materials fabricated by electric current activated sintering, Vacuum 137 (2017) 137-147.

[28] D. Fabrègue, J. Piallat, E. Maire, Y. Jorand, V. Massardier-Jourdan, G. Bonnefont, Spark plasma sintering of pure iron nanopowders by a simple route, Powder Metall. 55 (2012) 76-79.

[29] B. Srinivasarao, K. Oh-Ishi, T. Ohkubo, T. Mukai, K. Hono, Synthesis of high-strength bimodally grained iron by mechanical alloying and spark plasma sintering, Scr. Mater. 58 (2008) 759.

Accepted manuscript

ACCEPTED MANUSCRIPT

[30] X. Hong, A. Godfrey, C.L. Zhang, W. Liu, A. Chapuis, Investigation of grain subdivision at very low plastic strains in a magnesium alloy, Mater. Sci. Eng. A 693 (2017) 14-21.

[31] X. C. Liu, H. W. Zhang, K. Lu, Strain-Induced Ultrahard and Ultrastable Nanolaminated Structure in Nickel, Science 342 (2013) 337-340

[32] Q. A. Shaikh, Interdiffusion measurement of niobium and tantalum in iron base alloys, Mater. Sci. Technol. 6 (1990) 1177-1180.

[33] J. K. Mackenzie, Second Paper on Statistics Associated with the Random Disorientation of Cubes Biometrika 44 (1958) 205-210.

[34] Q. Contrepois, C. Maurice, J.H. Driver, Hot rolling textures of Al–Cu–Li and Al–Zn–Mg–Cu aeronautical alloys: Experiments and simulations to high strains, Mater. Sci. Eng. A 527 (2010) 7305-7312.

[35] A. Albou, J.H. Driver, C. Maurice, Microband evolution during large plastic strains of stable {1 1 0}<1 1 2> Al and Al-Mn crystals, Acta Mater. 58 (2010) 3022-3034.

[36] S. Van Boxel, M. Seefeldt, B. Verlinden, P. Van Houtte, Visualization of grain subdivision by analysing the misorientations within a grain using electron backscatter diffraction, J. Microsc. 218 (2005) 104-114.

[37] Z.C. Cordero, B.E. Knight, C.A. Schuh, Six decades of the Hall-Petch effect – a survey of grain size strengthening studies on pure metals, Int. Mater. Revs. 61 (2016) 494-512.

[38] J. C. M. Li, Y. T. Chou, Role of dislocations in in flow stress grain size relationships, Metall. Trans. 1 (1970) 1145-1159.

Accepted manuscript

ACCEPTED MANUSCRIPT

[39]] J. P. Hirth, Influence of grain-boundaries on mechanical properties, Metall. Trans. 3 (1972) 3047-3067.

[40] B. Mintz, Importance of Ky (hall-petch slope) in determining strength of steels, Metals Technol. 11 (1984) 265-272.

[41] W. B. Morrison, W. C. Leslie, The yield stress-grain size relation in iron substitutional alloys, Metall. Trans. 4 (1973) 379-381.

[42] E. O. Hall, The Deformation and Ageing of Mild Steel: III Discussion of Results, Proc. Phys. Soc. B 64 (1951) 747-753.

[43] R. Armstrong, I. Codd, R. M. Douthwaite, N. J. Petch, The plastic deformation of polycrystalline aggregates, Phil. Mag. 7 (1962) 45-58.

[44] W. B. Morrison, The effect of grain size on the stress-strain relationship in low-carbon steel, Trans. Am. Soc. Met. 59 (1966) 824-846.

[45] B. Mintz, H. Ke, G.D.W. Smith, grain-size strengthening in steel and its relationship to grain-boundary segregation of carbon, Materials Science and Technology 8(6) (1992) 537-540

[46] S. Gao, A. Shibata, M. Chen, N. Park, N. Tsuji, Correlation between continuous / discontinuous yielding and Hall-Petch slope in high purity iron, Mater. Trans. 55 (2014) 69-72.

[47] R. O. Scattergood, D. J. Bacon, The strengthening effect of voids, Acta Metall. 30 (1982) 1665-1677.

[48] J. S. H. Lake, Control of discontinuous yielding by temper rolling, J. Mech. Work. Technol. 12 (1985) 35-66.

Accepted manuscript

ACCEPTED MANUSCRIPT

[49] X. Fang, Z. Fan, B. Ralph, P. Evans, R. Underhill, Effect of temper rolling on tensile properties of C-Mn steels, Mater. Sci. Technol. 18 (2002) 285-288.

[50] J. Grassino, M. Vedani, G. Vimercati, G. Zanella, Effects of skin pass rolling parameters on mechanical properties of steels, Int. J. Precis. Eng. Manufac. 13 (2012) 2017-2026.

[51] X.L. Wu, M.X. Yang, F.P. Yuan, G.L. Wu, Y.J. Wei, X. Huang, Y.T. Zhu, Heterogeneous lamella structure unites ultrafine-grain strength with coarse-grain ductility, Proc. Nat. Acad. Sci. 112 (2015) 14501-14505.

[52] X.L. Wu, P. Jiang, L. Chen, F.P. Yuan, Y.T. Zhu, Extraordinary strain hardening by gradient structure, Proc. Nat. Acad. Sci. 111 (2014) 7197-7201

[53] Z. Zeng, X.Y. Li, D.S. Xu, L. Lu, H.J. Gao, T. Zhu, Gradient plasticity in gradient nano-grained metals, Extreme Mech. Lett. 8 (2016) 213-219.

Accepted manuscript

ACCEPTED MANUSCRIPT

Table 1: Initial powder composition (values given as wt%).

Cu	Si	Ni	Cr	Mg	Al	Ti
⩽0.005	⩽0.002	⩽0.002	⩽0.005	⩽0.004	⩽0.001	⩽0.005
Mo	Pb	Mn	Ca	Sn	Fe	
⩽0.004	⩽0.004	⩽0.003	⩽0.004	⩽0.008	⩾99.9	

Accepted manuscript

ACCEPTED MANUSCRIPT

Table 2: Density and samples prepared from powders P1, P2 and P3 with grain size for selected samples. Entries in bold indicate the samples used for mechanical and microstructural investigations in this study.

Powder	Sintering Temperature (°C)	Relative density (%)	Grain size (μm)	
			θ > 2°	θ > 15°
P1	650	94.60 ± 0.01	-	-
P1	**750**	**97.38 ± 1.19**	**1.0**	**1.1**
P1	850	97.45 ± 0.03	13	13
P1	950	97.48 ± 0.08	14	14
P2	**750**	**97.88 ± 0.63**	**2.6**	**2.7**
P3	750	91.79 ± 0.18	-	-
P3	800	92.36 ± 0.20	-	-
P3	850	93.18 ± 0.07	-	-
P3	900	95.38 ± 0.17	2.8	2.9
P3	950	96.22 ± 0.65	2.8	3.2
P3	**1000**	**96.35 ± 0.22**	**4.0**	**4.6**

Accepted manuscript

ACCEPTED MANUSCRIPT

Fig. 1: Scanning electron microscope images of the iron powders used in this investigation: (a) powder P1, (b) powder P2, and (c) powder P3.

Fig. 2: EBSD maps showing example microstructures for the samples used for mechanical testing with grain sizes (d_{2°) of: (a) 1 μm (EBSD step size 0.12 μm; SPS of powder P1 at 750 °C); (b) 2.6 μm (EBSD step size 0.12 μm; SPS of powder P2 at 750 °C); (c) 4.0 μm (EBSD step size 0.5 μm; SPS of powder P3 at 1000 °C); and (d) 33 μm (EBSD step size 1. 2 μm; rolled and annealed electrolytic iron). Silver and black lines indicate misorientations of >2° and >15°, respectively. Red lines indicate misorientations corresponding to a Σ3 relationship; inverse pole figure coloring superposed on a band contrast map.

Fig. 3: Misorientation distributions (2° bin size; 2° lower cut-off) for the investigated samples with grain sizes of: (a) 1 μm; (b) 2.6 μm; (c) 4.0 μm; and (d) 33 μm.

Fig. 4: Maps calculated from the EBSD data showing the misorientation angle (a-d) and misorientation axis in the sample reference frame (e-h) of each pixel to the grain average orientation for samples with grain size of: (a) 1 μm; (b) 2.6 μm; (c) 4.0 μm; and (d) 33 μm. The misorientation angle maps are scaled from 0° (yellow) to 2° (blue), with all misorientations angles >2° colored in green. For the misorientation axis ma the X axis is parallel to the sintering loading direction, and the Y axis is chosen at random in the sintering plane.

Fig. 5: Tensile flow curves for samples with grain sizes as indicated in the figure. Samples with grain sizes (d_{2°) of 1.0 μm, 2.6 μm, and 4.0 μm prepared from iron powders using SPS. The 2.6

Accepted manuscript

ACCEPTED MANUSCRIPT

μm, and 4.0 μm samples both show a yield drop and Lüders instability, followed by a similar high work-hardening rate.

Fig. 6: Scanning electron micrographs of the fracture surface of samples deformed in tension to failure for samples with grain size of: (a) 1 μm; (b) 2.6 μm; (c) 4.0 μm; and (d) 33 μm.

Fig. 7: Hall−Petch plot (inverse square root of the grain size, $d_{2^\circ}^{-0.5}$, against flow stress) for SPS samples with grain sizes of 1.0 μm, 2.6 μm, and 4.0 μm (solid squares) and rolled/annealed electrolytic iron with grain size 33 μm (hollow square). The solid line shows an extrapolation of the Hall-Petch parameters reported for Fe in a recent review paper [36]. The dashed lines show Hall-Petch plots taken from early studies on mild steel [43] (σ_0 = 70 MPa; k_{HP} = 740 MPaμm$^{0.5}$) and on low carbon steels [44] (σ_0 = 100 MPa; k_{HP} = 600 MPaμm$^{0.5}$).

Fig. 8: Tensile flow curves showing the effect of pre-compression deformation on the flow characteristics for the 2.6 μm grain size SPS material. The solid line shows the flow curve for the as-sintered material (reproduced from Fig. 5); the dotted and dashed lines show the flow curves for samples pre-compressed 5% perpendicular to and parallel to the tensile axis (TA), respectively. In both cases the yield point is removed with a corresponding large reduction in the flow stress.

Accepted manuscript

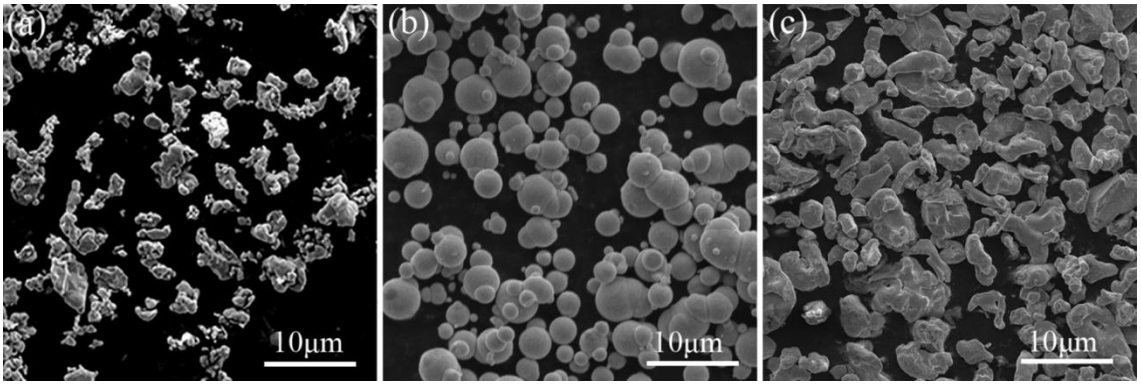

Fig. 1.

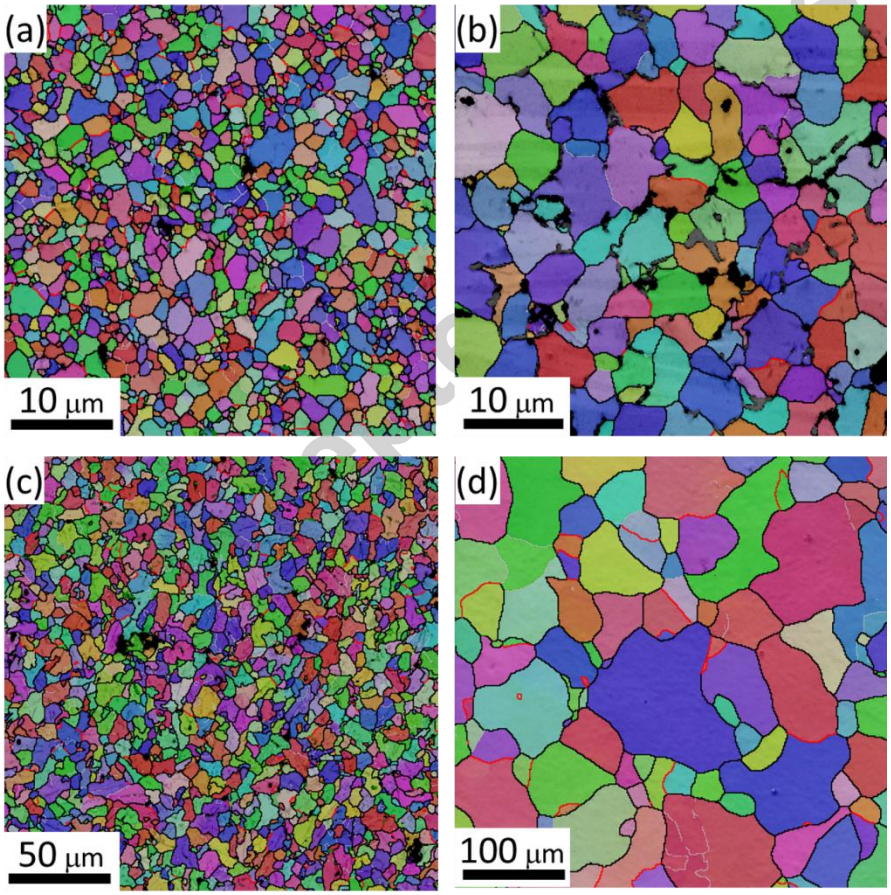

Fig. 2.

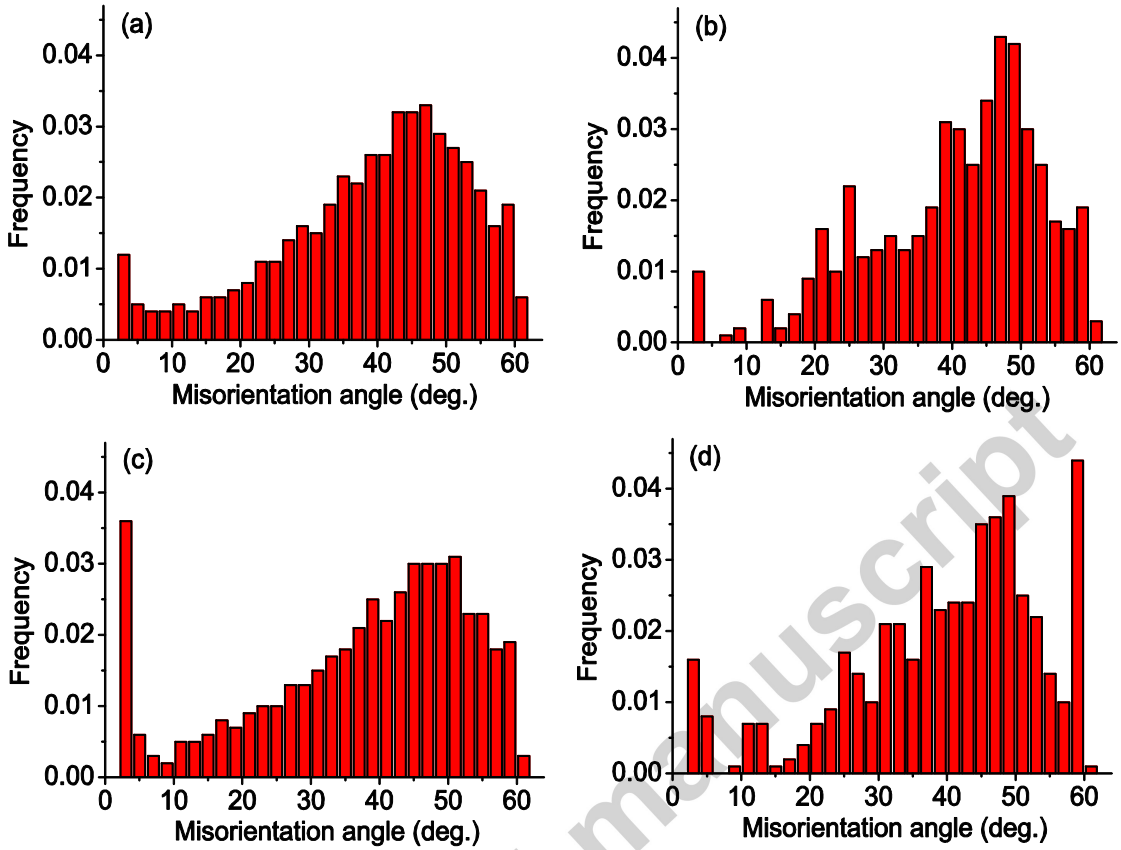

Fig. 3.

Accepted manuscript

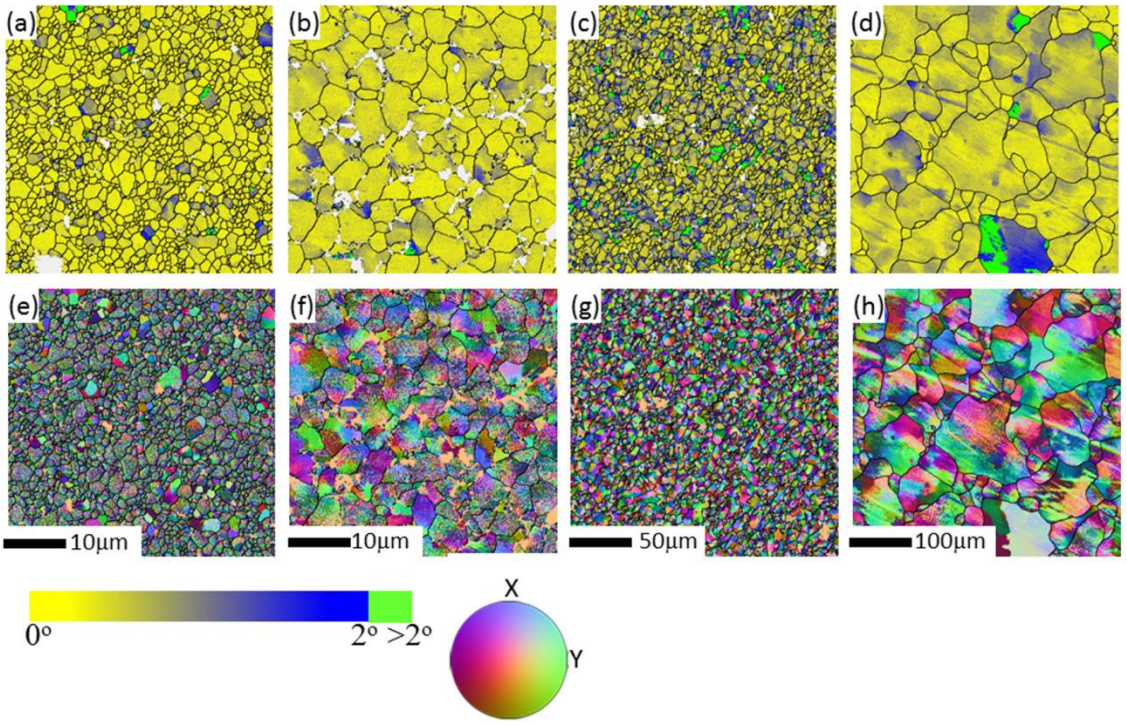
(a)
(b)
(c)
(d)
(e)
(f)
(g)
(h)
10μm
10μm
50μm
100μm
0°
2° >2°
X
Y

Fig. 4.

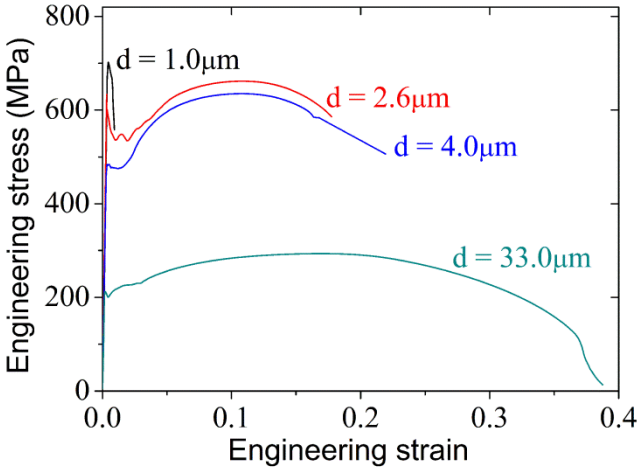
800
600
400
200
0
Engineering stress (MPa)
0.0
0.1
0.2
0.3
0.4
Engineering strain
d = 1.0μm
d = 2.6μm
d = 4.0μm
d = 33.0μm

Fig. 5.

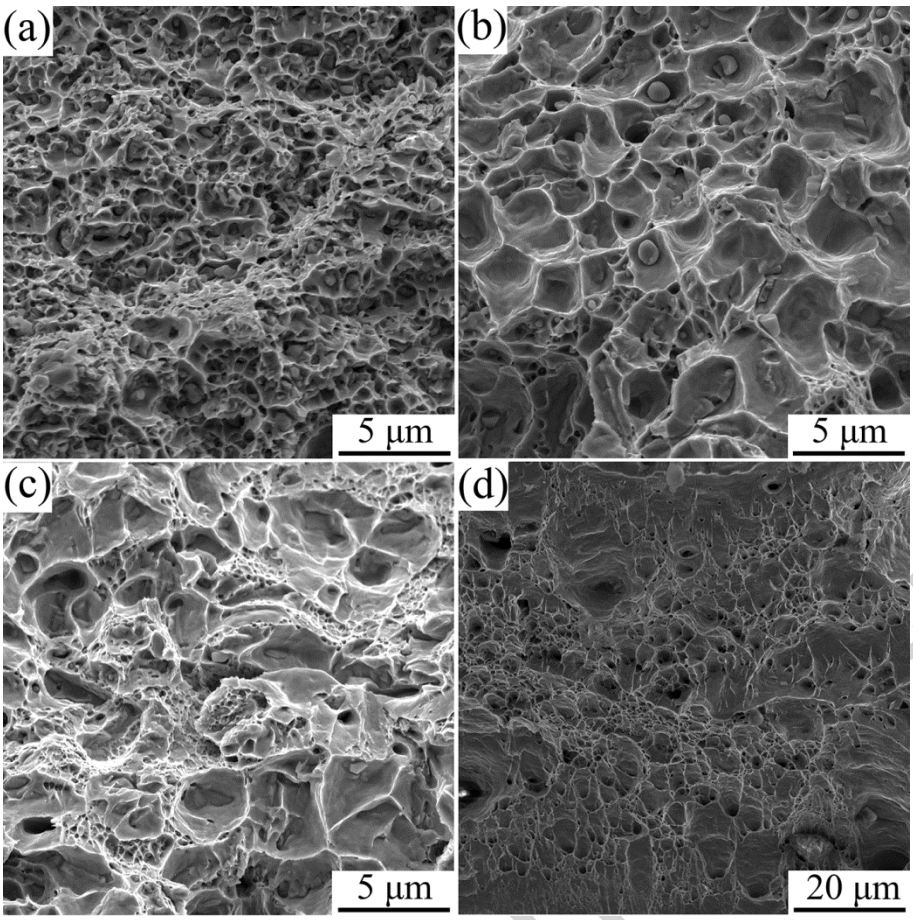

Fig. 6.

Accepted Manuscript

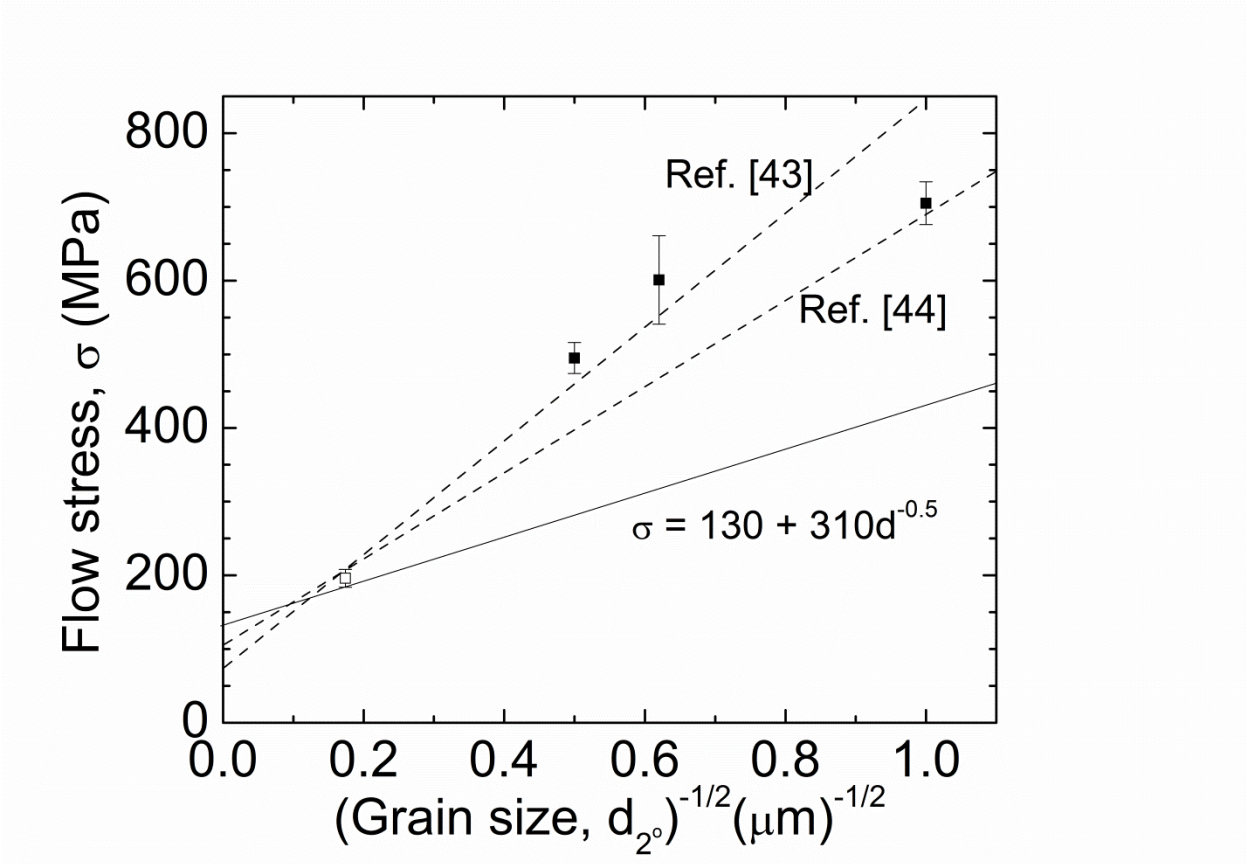
Flow stress, σ (MPa)
800
600
400
200
0
0.0
0.2
0.4
0.6
0.8
1.0
(Grain size, d2°)-1/2(μm)-1/2
Ref. [43]
Ref. [44]
σ = 130 + 310d-0.5

Fig. 7.

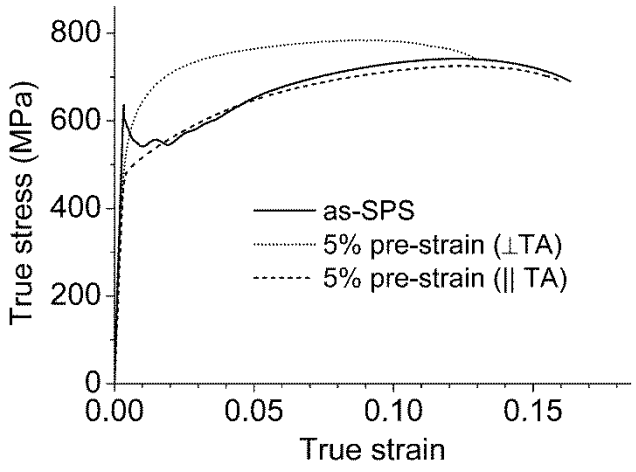
True stress (MPa)
800
600
400
200
0
0.00
0.05
0.10
0.15
True strain
as-SPS
5% pre-strain (⊥TA)
5% pre-strain (|| TA)

Fig. 8.